

Direct and compound reactions induced by unstable helium beams near the Coulomb barrier

A. Navin,¹ V. Tripathi,^{1,*} Y. Blumenfeld,² V. Nanal,³ C. Simenel,^{4,†} J. M. Casandjian,^{4,‡} G. de France,⁴ R. Raabe,^{5,§} D. Bazin,⁶
 A. Chatterjee,¹ M. Dasgupta,⁷ S. Kailas,¹ R. C. Lemmon,⁸ K. Mahata,¹ R. G. Pillay,³ E. C. Pollacco,⁵ K. Ramachandran,¹
 M. Rejmund,⁴ A. Shrivastava,¹ J. L. Sida,^{5,||} and E. Tryggestad²

¹*Nuclear Physics Division, Bhabha Atomic Research Centre, Mumbai 400085, India*

²*Institut de Physique Nucléaire, IN2P3-CNRS, F-91406, Orsay Cedex, France*

³*Department of Nuclear and Atomic Physics, Tata Institute of Fundamental Research, Mumbai 400005, India*

⁴*GANIL, Boîte Postale 5027, F-14076, Caen Cedex, France*

⁵*DSM/DAPNIA/SPhN, CEA Saclay, F-91191, Gif-sur-Yvette Cedex, France*

⁶*National Superconducting Cyclotron Laboratory, Michigan State University, East Lansing, Michigan 48824, USA*

⁷*Department of Nuclear Physics, Australian National University, Canberra, Australian Capital Territory 0200, Australia*

⁸*CRLC, Daresbury Laboratory, Daresbury, Warrington, WA4 4AD, United Kingdom*

(Received 26 August 2003; revised manuscript received 1 June 2004; published 6 October 2004)

Reactions induced by radioactive ${}^{6,8}\text{He}$ beams from the SPIRAL facility were studied on ${}^{63,65}\text{Cu}$ and ${}^{188,190,192}\text{Os}$ targets and compared to reactions with the stable ${}^4\text{He}$ projectiles from the Mumbai Pelletron. Partial residue cross sections for fusion and neutron transfer obtained from the measured intensities of characteristic in-beam γ rays for the ${}^6\text{He}+{}^{63,65}\text{Cu}$ systems are presented. Coincidence measurements of heavy reaction products, identified by their characteristic γ rays, with projectilelike charged particles, provide direct evidence for a large transfer cross section with Borromean nuclei ${}^6\text{He}$ at 19.5 and 30 MeV and ${}^8\text{He}$ at 27 MeV. Reaction cross sections were also obtained from measured elastic angular distributions for ${}^{6,8}\text{He}+\text{Cu}$ systems. Cross sections for fusion and direct reactions with ${}^{4,6}\text{He}$ beams on heavier targets of ${}^{188,192}\text{Os}$ at 30 MeV are also presented. The present work underlines the need to distinguish between various reaction mechanisms leading to the same products before drawing conclusions about the effect of weak binding on the fusion process. The feasibility of extracting small cross sections from inclusive in-beam γ -ray measurements for reaction studies near the Coulomb barrier with low intensity isotope separation on-line beams is highlighted.

DOI: 10.1103/PhysRevC.70.044601

PACS number(s): 25.60.Pj, 25.60.Je, 25.70.Jj

I. INTRODUCTION

Nuclei far from stability, characterized by small binding energies and large values of isospin, exhibit a variety of novel properties like extended wave function(s) of the valence nucleon(s), a Borromean structure (a three-body bound system, where any of its two-body subsystems are unbound), and large breakup probabilities. These features are expected to strongly affect the reactions with radioactive ion beams (RIBs) especially at energies near the Coulomb barrier (V_b) [1]. The recent advent of facilities using the isotope separation on-line (ISOL) technique has opened up new opportunities to measure and understand reactions with low intensity RIBs at energies near V_b .

Fusion studies with radioactive ion beams are currently investigating the conflicting results/predictions of the influ-

ence of weak binding of the projectile. The larger radii of such nuclei and the coupling to low lying resonant states should tend to enhance the fusion cross section. However, predictions regarding the influence of the strong breakup channels in these weakly bound systems on fusion have been controversial. In a simple picture it could lower the fusion cross section (as compared to a one-dimensional barrier penetration model) due to loss of flux in the entrance channel. Contrary to this is the expectation that strong coupling to the breakup channel would enhance the fusion cross section below the Coulomb barrier. These contradictory predictions have been theoretically reconciled in Ref. [2], where using the ${}^{11}\text{Be}+{}^{208}\text{Pb}$ system, it is shown that the effect of coupling to continuum states is to enhance the complete fusion cross sections below the barrier and reduce it above the barrier. Complete fusion is the total amalgamation of the target and projectile. In practice, interpretation of complete fusion with these neutron-rich weakly bound nuclei is difficult, both experimentally and theoretically, due to the occurrence of several different reactions at energies near the barrier, which result in products which can be misinterpreted as complete fusion. Inelastic scattering results in the excitation of the target and/or projectile without any mass transfer. Transfer is the direct exchange of one (or several) nucleons between projectile and target. The weak binding of these projectiles leads to a significant cross section for both elastic breakup, transfer reactions and/or breakup followed by capture of a part of it by the target. The latter process is also referred to as incomplete fusion, massive transfer or breakup/stripping.

*Present address: Department of Physics, Florida State University, Tallahassee, Florida 32306, USA.

†Present address: DSM/DAPNIA/SPhN, CEA Saclay, F-91191, Gif-sur-Yvette Cedex, France.

‡Present address: DSM/DAPNIA/SAP, CEA Saclay, F-91191 Gif-sur-Yvette Cedex, France.

§Present address: Instituut voor Kern-en Stralingsfysica, University of Leuven, B-3001 Leuven, Belgium.

||Present address: CEA/DAM/DPTA/SPN, 91680 Bruyères le Châtel, France.

Investigations of the fusion process have been made with stable weakly bound ${}^6,7\text{Li}$ [3–5] and ${}^9\text{Be}$ [6–8] beams and radioactive beams of ${}^6\text{He}$ [9,10], ${}^{7,10,11}\text{Be}$ [11,12], ${}^{17}\text{F}$ [13], ${}^{29,31}\text{Al}$ [14], and ${}^{38}\text{S}$ [15]; however, with differing conclusions about fusion enhancement/suppression, when compared with measurements with stable isotopes and/or coupled channel calculations [2,16,17]. This discrepancy arises mainly from the difficulty in interpreting the experimental results with weakly bound nuclei, due to the additional contributions to the cross section, arising from noncompound processes discussed above which cannot be differentiated in all cases.

In interactions of light neutron-rich radioactive beams with medium mass targets, reaction products formed in fusion evaporation and other direct reactions mentioned above could be the same, due to the preponderance of charge particle emission from the compound system. This is not the case with heavier compound systems which decay mainly by the emission of neutrons (it may be difficult to differentiate between fusion-fission and transfer induced fission in fissile systems). Therefore, before interpreting results of fusion cross section measurements with weakly bound projectiles, it is of paramount importance to ensure that the quoted fusion cross section does not contain contributions from other mechanisms. Striving toward a comprehensive understanding of low energy reactions with weakly bound projectiles thus entails performing experiments to separate the different mechanisms and measure their respective cross sections.

A related issue is connected to exclusive studies of nucleon transfer with radioactive ion beams. Such measurements are relatively sparse [18,19], due to the experimental limitation in disentangling elastic breakup and transfer. Studies of transfer reactions, with Borromean nuclei, could provide a useful probe to understand pairing in finite fermion systems, like those in metal clusters, fullerenes, and superconductors [20]. It is important to measure neutron transfer cross sections and then try to understand the relative importance of breakup and transfer on the fusion process within a coupled channel framework. Only estimates of neutron transfer have been attempted from the measurement of α particles in ${}^6\text{He}$ induced reactions [21,22]. The ambiguity in the interpretation of the origin of the measured inclusive α particles has been recently discussed [23].

With light projectiles at low incident energies, direct detection of residues is extremely difficult due to their low recoil velocities. Therefore, investigations of fusion cross sections have focused on prompt measurements through fission fragments [10,11] or γ rays [3,5] or measurements through decay α particles [4,9,14] or x-ray activity [22]. These techniques yield precise measurements of the cross section for various residues (except in the case of fission measurements, where only a total fission cross section is obtained). However, the separation of the different reaction mechanisms is often ambiguous as several mechanisms can populate the same nucleus. A complementary approach to obtain direct reaction cross sections has been the measurement of light charged particle spectra for projectiles of ${}^6\text{He}$ [21,22], ${}^{6,7,8}\text{Li}$ [24–26], and ${}^9\text{Be}$ [27]. These studies are sensitive to elastic breakup, which is not observed in the residue measurements, but cannot distinguish between breakup,

transfer, and incomplete fusion. Very recently for the ${}^6\text{He}+{}^{64}\text{Zn}$ system, both residue and inclusive alpha particle measurements have been reported [22]. In the present work we have attempted to obtain a more complete understanding of low energy reactions induced by the neutron-rich Borromean nuclei ${}^{6,8}\text{He}$, on both medium mass ${}^{63,65}\text{Cu}$ and heavy ${}^{188,190,192}\text{Os}$ targets, by relying on a model independent comparison with ${}^4\text{He}$ induced reactions. In the case of the ${}^6\text{He}$ beam inclusive prompt γ -ray measurements have been performed in order to obtain residue cross sections (fusion and neutron transfer), and for the first time in a radioactive beam experiment, coincident measurements between γ rays and light charged particles have been attempted to address the separation of fusion and neutron transfer mechanisms. In the case of ${}^8\text{He}$, the weak beam intensity and the presence of large background from ${}^8\text{He}$ β^- decay precluded a successful singles measurement; however, coincidences between the charged particles and characteristic γ rays could be observed. Additionally, elastic scattering angular distributions were measured and analyzed for both projectiles to obtain the reaction cross-section. In the case of the very tightly bound ${}^4\text{He}$ projectiles, direct processes are expected to be weak in the energy range studied, and only γ -ray singles were measured to obtain the complete fusion cross sections.

In the next section the experimental details are given, followed in Sec. III by a detailed description of the analysis of the data to distinguish reaction products arising from compound and transfer processes, the main highlight of this work. The extraction of the reaction cross sections from the elastic scattering measurements allows us additionally to infer breakup cross sections through a subtraction procedure. The results for the medium mass targets along with those for heavier targets, and their differences are then discussed. The important implications of the large transfer reaction contribution to the measured residue cross section are discussed in Sec. IV followed by a summary of the work.

II. EXPERIMENTAL DETAILS

The measurements with ${}^4\text{He}$ beams, were made at the 14UD BARC-TIFR Pelletron Accelerator Mumbai, in the energy range 16 to 34 MeV. The intensities of the low lying characteristic γ rays from the evaporation residues (ER's) were measured, using four efficiency calibrated Compton suppressed clover detectors, to obtain the complete fusion cross sections [3,5]. The thickness of the rolled enriched ${}^{63}\text{Cu}$ and ${}^{65}\text{Cu}$ targets of 2.8 mg/cm² and 3.2 mg/cm², respectively, were obtained both by weighing and by measuring the energy loss for alpha particles. Isotopically enriched targets of ${}^{188,190,192}\text{Os}$ having a target thickness of 1.60 mg/cm², 1.04 mg/cm², and 640 $\mu\text{g}/\text{cm}^2$, respectively, were prepared by electrodeposition on ≈ 1 mg/cm² Cu backings [28]. The target thicknesses were estimated by measuring the Rutherford scattering cross sections and also using the tracer method discussed in [28]. While the ${}^{190,192}\text{Os}$ targets were 99% enriched, the ${}^{188}\text{Os}$ had the following isotopic composition: 86.7%, 9.51%, 2.46%, and 1.33% of ${}^{188,189,190,192}\text{Os}$, respectively. The beam current was measured in a 1 m long Faraday cup placed after the target.

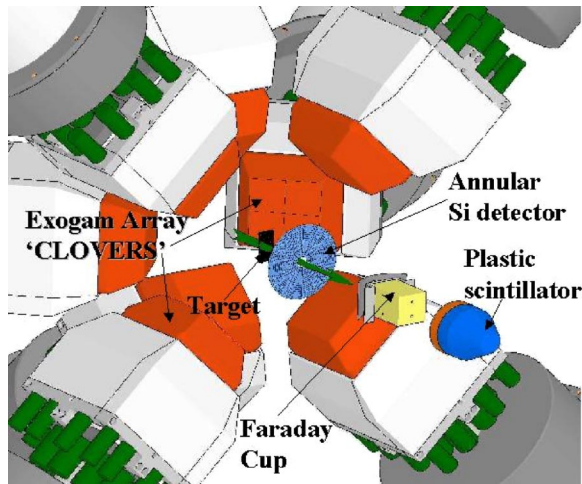


FIG. 1. (Color online) Schematic of the experimental setup at SPIRAL. The Faraday cup (plastic detector) was used for monitoring the beam particles with the ${}^6\text{He}$ (${}^8\text{He}$) beam.

Radioactive beams, ${}^6,8\text{He}$, were obtained from the recently commissioned ISOL facility, SPIRAL at GANIL [29]. The fragmentation of a 75 MeV/nucleon ${}^{13}\text{C}$ beam on a thick graphite target was used to produce the ${}^6,8\text{He}$ ions which were accelerated by the CIME cyclotron to 19.5 and 30 MeV for ${}^6\text{He}$ and 27 MeV for ${}^8\text{He}$ (typical energy resolution $\Delta E/E \sim 10^{-3}$). The ${}^6\text{He}$ and ${}^8\text{He}$ beams, with beam spot size of 5 mm and 8 mm full width at half maximum, respectively, had average intensities of 1×10^7 particles/s and 7×10^4 particles/s. The intensity of the ${}^6\text{He}$ was measured using a Faraday cup with a current amplifier while a plastic scintillator of 2 in. diameter was used to directly count the ${}^8\text{He}$ beam particles, the intensity being too low to be reliably measured with the Faraday cup. The electronic stability of the current amplifier for a given measurement was better than 1%. With the unstable beams of He, data from the following reactions will be reported: ${}^6\text{He} + {}^{63}\text{Cu}$ at 30 MeV; ${}^6\text{He} + {}^{65}\text{Cu}$ at 19.5 and 30 MeV; ${}^8\text{He} + {}^{63}\text{Cu}$ at 27 MeV; and ${}^6\text{He} + {}^{188,190,192}\text{Os}$ at 30 MeV.

The characteristic γ rays from the heavy reaction products produced in the reactions with ${}^6,8\text{He}$ were detected using eight clover detectors of the EXOGAM array [30] placed at a distance of 10.5 cm from the target. The charged particles were detected in a 500 μm thick annular Si detector (active inner and outer diameters of 22 mm and 70 mm, respectively, with 16 rings and 16 sectors), placed at distance of 3.5 cm downstream from the target. The energy resolution for 30 MeV ${}^6\text{He}$ nuclei was ≈ 300 keV. Some of the rings of this detector malfunctioned during the experiment, inducing gaps in the measured angular distributions. A schematic of the setup used at SPIRAL is shown in Fig. 1.

Figure 2(a) displays the inclusive γ -ray spectra from the ${}^6\text{He} + {}^{65}\text{Cu}$ reaction at 19.5 MeV. These spectra are the sum of the spectra for all individual clovers operated in add-back mode. The bottom spectrum shows the significant reduction of the background obtained by gating on the peak of the time spectrum taken between the clovers and the CIME rf.

The intensities of the well studied low lying γ transitions extracted from the measured inclusive γ -ray spectra were

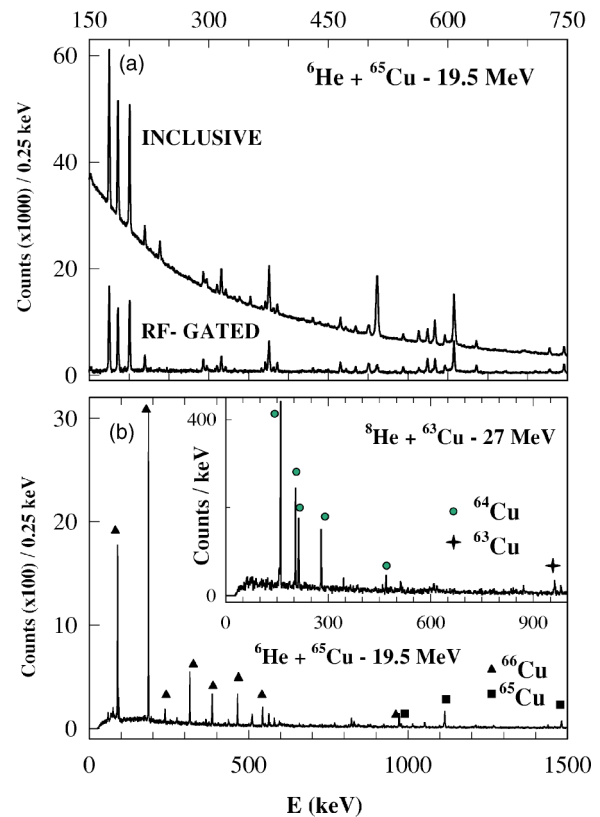


FIG. 2. γ -ray spectra for ${}^6,8\text{He} + {}^{63,65}\text{Cu}$. (a) Inclusive spectrum for ${}^6\text{He} + {}^{65}\text{Cu}$ at 19.5 MeV and the spectrum gated with the pulsed beam showing the suppression of the background. All dominant peaks are identified. (b) Spectra in coincidence with charged particles detected in the annular Si detector for ${}^6,8\text{He}$. The lines corresponding to targetlike products (arising from neutron transfer followed by evaporation) are labeled.

used to obtain the partial residue cross sections for the ${}^4,6\text{He} + {}^{65}\text{Cu}$ systems which are shown in Figs. 3(a) and 3(b), respectively. The corrections, due to direct population of the ground states which is not accompanied by γ -ray emission, are expected to be small due to low spins of the nearby lying levels and have not been considered. The fusion cross section is obtained from the sum of the cross sections for the various residues. The same procedure was followed to obtain the cross sections for the ${}^4,6\text{He} + {}^{63}\text{Cu}$ systems which are shown in Fig. 4(a) and 4(b), respectively.

For the fusion of ${}^4,6\text{He}$ with the isotopes of Os, the cross sections for the even-even ER's were extracted from the extrapolated value of the intensity at $J=0$, obtained from the measured γ -ray intensities for various transitions in the ground state rotational band [3]. Cross sections for the population of the odd-even ER's were obtained from the sum of the intensities of all the low lying transitions directly feeding the ground state. For the case of the ${}^4\text{He}$ beam, the total cross section was a sum of $2n$, $3n$, and $4n$ channels. In the case of the ${}^{188}\text{Os}$, corrections for the target impurities were made using both the statistical model and measured intensities of gamma transitions in nuclei produced solely by the impurities [31]. The fusion cross sections with the ${}^6\text{He}$ beams with Os isotopes at 30 MeV were obtained from the measured cross section for the $4n$ channel. The small cross section of

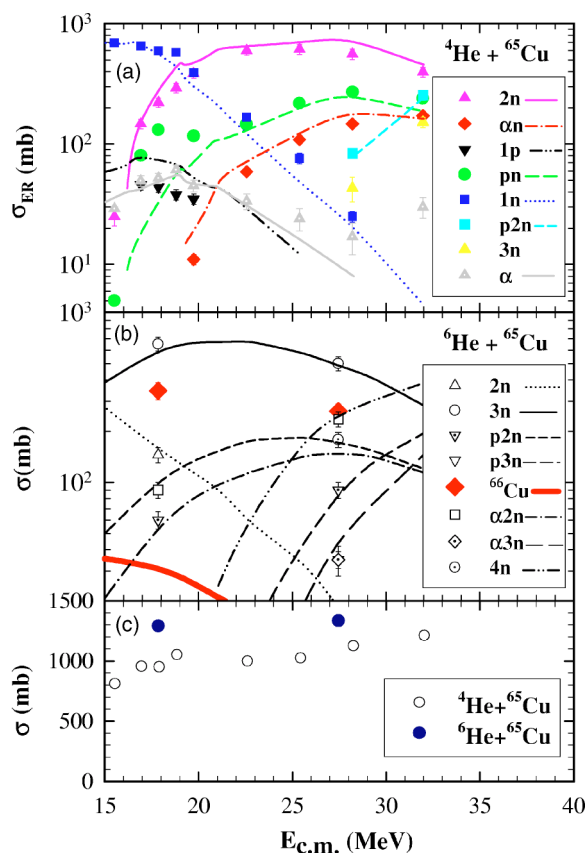


FIG. 3. (Color online) (a) Measured partial residue cross sections indicated by different symbols for ${}^4\text{He}+{}^{65}\text{Cu}$ system as a function of the center of mass energy. The lines are obtained using the statistical model code CASCADE (see text). (b) Same as in (a) for the ${}^6\text{He}+{}^{65}\text{Cu}$ system. (c) Total residue cross section for ${}^4\text{He}+{}^{65}\text{Cu}$ (open symbols) and ${}^6\text{He}+{}^{65}\text{Cu}$ (filled symbols). Only statistical errors are shown.

the $3n$ channel was not measured but was estimated from the statistical model CASCADE [32] using the same parameters that explained the partial cross sections for the measured α +Os systems and added to the measured $4n$ cross section in order to obtain the total residue cross section. The $3n$ contributions amounted to 22% and 5% of the fusion cross section for the ${}^{188}\text{Os}$ and ${}^{192}\text{Os}$ targets, respectively. The errors in the total cross sections arising from the measurements of the beam current, γ -ray efficiency, and target thickness and knowledge of the spectroscopic information of the residues have been estimated to be between 10% and 15% for the various projectile target combinations.

As can be seen from Figs. 3(b) and 4(b), absolute cross sections down to a few millibarns have been obtained from inclusive γ -ray measurements with a RIB, in this case ${}^6\text{He}$, for the first time. Such measurements are difficult primarily due to the presence of large background in the γ -ray spectra as has been discussed in Refs. [33,34]. However, the determination of absolute fusion cross sections in the present work demonstrates the wide applicability of this technique for nuclear reaction studies with low intensity RIB's and thin targets at energies near V_b . Use of this technique expands the scope of measuring fusion cross sections with RIB's involving lighter targets. Measurements until now had been mainly

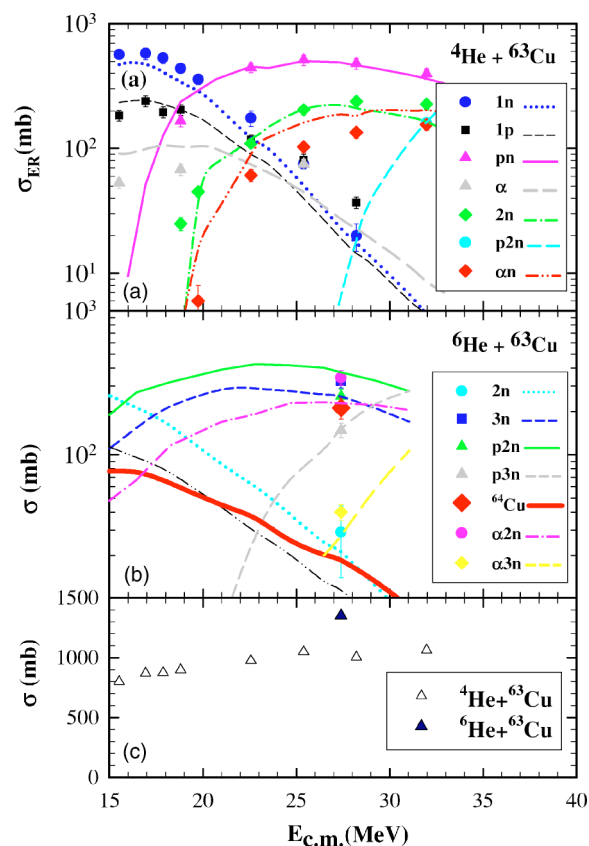


FIG. 4. (Color online) (a) Measured partial residue cross sections indicated by different symbols for ${}^4\text{He}+{}^{63}\text{Cu}$ system as a function of the center of mass energy. The lines are obtained using the statistical model code CASCADE (see text). (b) Same as in (a) for the ${}^6\text{He}+{}^{63}\text{Cu}$ system. (c) Total residue cross section for ${}^4\text{He}+{}^{63}\text{Cu}$ (open symbols) and ${}^6\text{He}+{}^{63}\text{Cu}$ (filled symbols). Only statistical errors are shown.

restricted to fusion with heavy targets. As the EXOGAM array was still in an early stage of implementation a configuration with only partial Compton shielding, which permitted a higher efficiency at the expense of lower peak to total ratio [30], was used. The present work not only pushed down the usable intensity limit as compared to earlier works [33] by two orders of magnitude but also absolute cross sections were obtained from inclusive spectra using low energy ISOL beams of ${}^6\text{He}$. Measurements using a low energy ${}^8\text{He}$ beam three orders of magnitude lower in intensity than the ${}^6\text{He}$ were extremely challenging. Due to the insufficient peak to background ratio, it was not possible to exploit the singles data even when gated by the CIME rf. Based on the present work, with improved Compton suppression (hence also active shielding of the backgrounds) and the full array, singles γ -ray measurements with even lower intensities will be possible. Measuring detailed fusion excitation functions around the barrier with RIB's is of course one of the goals of experimental programs such as this. We attempted such measurements for ${}^6\text{He}$, but were unsuccessful due to the difficulty of obtaining degraded beams of sufficient quality and intensity. Retuning the CIME cyclotron at several energies would have required a much longer beam time allocation.

With the aim of deducing total reaction cross sections, measurements of elastic scattering angular distributions were

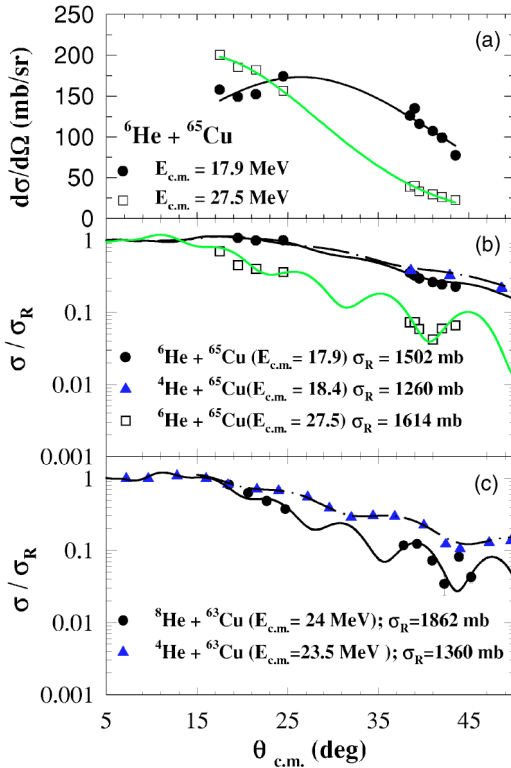


FIG. 5. (Color online) (a) α -particle angular distributions in coincidence with the 185.9 keV γ transition in ^{66}Cu for $^6\text{He} + ^{65}\text{Cu}$. The lines are Gaussian fits to the data. (b) Elastic angular distributions for $^6\text{He} + ^{65}\text{Cu}$ and for $^4\text{He} + ^{65}\text{Cu}$ (Ref. [42]). The lines are calculations using ECIS97. (c) Same as in (b) for $^8\text{He} + ^{63}\text{Cu}$ and $^4\text{He} + ^{63}\text{Cu}$ (Ref. [43]). Only statistical errors are indicated.

performed for the $^6\text{He} + ^{65}\text{Cu}$ system at 19.5 MeV and 30 MeV and the $^8\text{He} + ^{63}\text{Cu}$ system at 27 MeV. The angular range between 15° and 50° was covered and the measured angular distributions are shown in Fig 5. The statistical errors are indicated in the angular distributions. For each reaction Monte Carlo simulations, taking into account the finite size of the beam and the detailed geometry of the detector, were used to obtain the center of mass angle and solid angle corresponding to each ring and sector. The simulation provided the number of events and their expected energy, from a set of events generated following Rutherford distributions for the different cases. The effects of energy and angular straggling in the targets were also taken into account in the simulation. The results of the simulation were checked through elastic scattering measurements on Os and W targets, where the elastic cross section at 19.5 MeV for the angles measured follows Rutherford scattering.

III. ANALYSIS AND RESULTS

A. Products from direct and compound process in medium mass targets

As mentioned in Sec. I, for reactions induced by light neutron-rich projectiles, there exists an ambiguity between the products of fusion and those from direct reactions. In this section, we present evidence to show that in reactions with

weakly bound isotopes of He, direct reactions (neutron transfer in this case) occur with a large probability and result in products which could erroneously be attributed to fusion. First we compare the cross sections of reaction products with statistical model calculations and deduce that the abnormally large cross section for a few specific channels is incompatible with the fusion process. We then show that the energy spectra and angular distributions of the charged particles measured in coincidence with these channels are consistent with those of a neutron transfer mechanism.

1. Statistical model analysis

Figure 3(a) shows the residue cross sections as a function of the center of mass energy for the $^4\text{He} + ^{65}\text{Cu}$ system. The lines in the figure are statistical model calculations for the evaporation residues formed in decay of ^{69}Ga with the code CASCADE [32]. The level density formalism of Ignatyuk *et al.* [35], with a level density parameter $a=A/9$ was used. The transmission coefficients were taken from Refs. [36–38] for the neutron, proton, and alpha particles, respectively. A Woods-Saxon shape was chosen for the angular momentum distribution with a diffuseness of $2\hbar$ and l_{max} assuming a barrier height and radius calculated from systematics. As can be seen from the figure, the various partial cross sections are reasonably well explained by the statistical model.

The *same set* of parameters was used to predict the partial cross sections for the $^6\text{He} + ^{65}\text{Cu}$ system which are shown in Fig. 3(b). Once again, a good account of the partial residue cross sections is obtained *except* for the α -n evaporation channel (^{66}Cu residue). This discrepancy between the measured (filled diamond) and calculated (thick curve) cross sections for ^{66}Cu is unexpected in a compound nucleus picture, where ^{66}Cu would not survive, as it would be sufficiently excited to emit more particles. Hence the large cross section for ^{66}Cu must have an origin different from fusion evaporation.

Similar results and calculations are shown for the ^{63}Cu target (Fig. 4), albeit only for the highest ^6He energy. Again, the ^4He data are well reproduced. The only strong departure from the statistical model calculation in the case of the $^6\text{He} + ^{63}\text{Cu}$ system is for the production of ^{64}Cu , α -n channel, as can be seen from Fig. 4(b), reinforcing the evidence for a large noncompound contribution to these reactions.

2. Particle-gamma correlations

a. ^6He . The large production cross sections for ^{66}Cu discussed above in the $^6\text{He} + ^{65}\text{Cu}$ reactions can be further investigated through particle- γ coincidence events. Fig. 2(b) shows the γ -ray spectrum measured in coincidence with any charged particle detected in the Si detector for the reaction at 19.5 MeV. It is seen to be dominated by transitions in ^{66}Cu . A representative charged particle spectrum in coincidence with the 185.9 keV γ rays from the first excited state in ^{66}Cu is shown in Fig. 6(a) (full line). These charged particles can be identified with alpha particles since they are in coincidence with the γ ray from the decay of the first excited state of ^{66}Cu , which is an α -n channel. This spectrum peaks near $Q=0$ which is consistent with the semiclassical matching

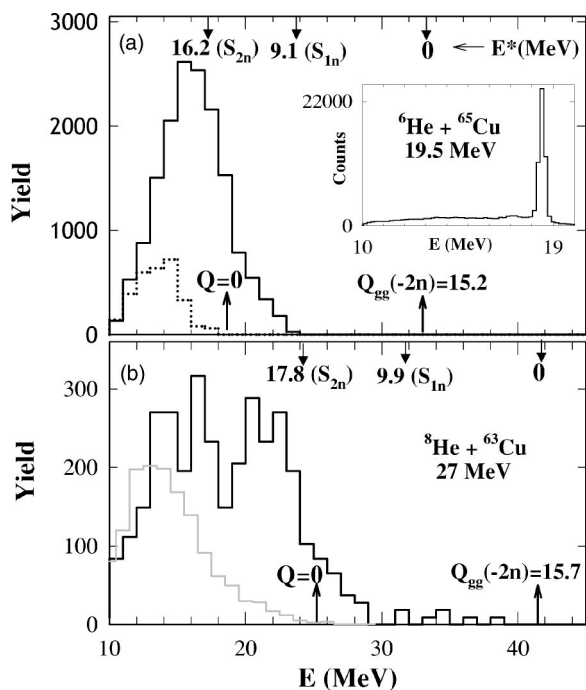


FIG. 6. Charged particles measured in the annular Si detector. (a) In coincidence with the 185.9 keV γ transition in ^{66}Cu (full line) and 1115.5 keV in ^{65}Cu (dotted line) for $^6\text{He} + ^{65}\text{Cu}$ at 19.5 MeV at $\theta_{lab} = 35^\circ$. The yields have been corrected for efficiency and branching of the gating transition. Inset shows the corresponding inclusive spectrum. (b) $^8\text{He} + ^{63}\text{Cu}$ at 27 MeV gated by the 159.1 keV transition in ^{64}Cu at $\theta_{lab} = 37^\circ$. The gray curve is a calculated α evaporation spectrum using a statistical model. The ground state Q values (Q_{gg}) and the neutron separation energies (S_n) in the residual nucleus in a two-neutron stripping reaction are indicated.

condition for neutron transfer (expected to peak near $Q = Q_{opt} = 0$) [39].

Considering the large spectroscopic factor for the $\alpha + 2n$ configuration of the ground state of ^6He [40,41] this spectrum is interpreted as arising from a $2n$ transfer leading to α and $^{67}\text{Cu}^*$. As seen from Fig. 6(a), the peak of the Q -value spectrum is well above the one-neutron threshold S_{1n} in ^{67}Cu and is consistent with the observed large cross section for the $1n$ emission channel ^{66}Cu and the absence of ^{67}Cu [Fig. 3(b)]. The population of ^{65}Cu expected for excitation energies above S_{2n} , confirmed by the observed Q -value spectrum gated by the 1115.1 keV γ rays from ^{65}Cu , is displayed as a dotted curve in Fig. 6(a). Thus, these measured Q -value spectra are consistent with a two-neutron transfer followed by evaporation. Given the unbound nature of ^5He , these results could be also explained by contributions from both $1n$ and $2n$ transfer. Only a direct measurement of the energies and angular distributions of the emitted neutrons could lead to an assessment of the relative contributions of one-neutron and two-neutron transfer.

The interpretation of the Q -value spectrum in terms of direct transfer is further supported by the angular distributions for α particles in coincidence with γ rays from the first excited state of ^{66}Cu which are shown in Fig. 5(a). Despite the fragmentary nature of these distributions, due to the missing ring signals of the silicon detector, the angular dis-

tribution at $E_{lab} = 19.5$ MeV is seen to peak near the grazing angle, while that at 30 MeV is forward peaked. Both angular distributions are again consistent with those expected for a direct transfer process though, at 30 MeV no measurements were taken below the grazing angle.

The total neutron transfer cross sections were obtained from the measured intensities from the inclusive gamma-ray spectra and were corrected for the small compound nuclear contributions to ^{66}Cu at 19.5 MeV calculated with the code CASCADE. The transfer cross sections for the $^6\text{He} + ^{65}\text{Cu}$ system at 19.5 and 30 MeV are 355 ± 30 mb and 335 ± 50 mb respectively.

b. ^8He . The inset of Fig. 2(b) displays the γ -ray spectrum from the $^8\text{He} + ^{63}\text{Cu}$ reaction at 27 MeV in coincidence with charged particles in the annular detector, which in this case can be either ^4He or ^6He . Similar to the case of $^6\text{He} + ^{63}\text{Cu}$, the spectrum is dominated by γ rays from ^{64}Cu . The Q -value spectrum for the $^8\text{He} + ^{63}\text{Cu}$ system at 27 MeV in coincidence with the 159.1 keV transition to the ground state in ^{64}Cu is shown in Fig. 6(b). The spectrum is broader than for the ^6He case and can be understood as consisting of two components. The high energy part has characteristics similar to those discussed for the $^6\text{He} + ^{63,65}\text{Cu}$ systems earlier and is thus consistent with $2n$ transfer followed by neutron evaporation. The additional strength at lower energy can be explained by α particles arising from compound nuclear evaporation. Indeed, the low energy part is in reasonable agreement with statistical model predictions for α particles emitted from the compound system [shown by the dotted histogram in the Fig. 6(b)]. (Another theoretically [41] possible origin of the low energy part could be alpha particles arising from a $4n$ transfer to the target; however, this cannot be quantified in this experiment due to lack of particle identification.) Due to the large γ background from the β^- decay of the ^8He beam to excited states in Li in the singles γ spectra no reliable values of absolute cross sections for the neutron transfer could be obtained for this system.

The present measurements of the characteristic γ rays from heavy products in coincidence with projectilelike charged particles for $^{6,8}\text{He}$ along with the statistical model analysis presented are a direct evidence for the large transfer cross sections with radioactive beams at energies near the Coulomb barrier.

3. Estimate of breakup cross sections for the ^6He beam

An important contribution to the reaction cross section induced by ^6He is the direct breakup of the projectile into α particles and neutrons, which are not captured by the target. The limited coverage and particle identification capability of the silicon detector precluded us from performing a direct measurement of the total α -particle cross section. Therefore, we have inferred the breakup cross section as the difference between the total reaction cross section and the total residue cross section, which, as shown above, consists of both fusion and transfer.

The reaction cross sections with ^6He beams were obtained from the measured elastic scattering angular distributions at 19.5 and 30 MeV and are given in Fig. 5(b). The reaction cross sections for the ^4He beam are quoted from previous

works [42,43]. The reaction cross sections were obtained for ${}^6\text{He}$ by fitting the angular distribution [Figs. 5(b) and 5(c)] using ECIS97 [44] with real and imaginary potentials having a geometry similar to Refs. [42,43]. For example, in the ${}^6\text{He}+{}^{65}\text{Cu}$ system at 30 MeV, the parameters for the depth, radius, and diffuseness of the real and imaginary part of the nuclear potential were 118.7 MeV, 1.13 fm, and 0.47 fm and 25.4 MeV, 1.194 fm, and 0.158 fm, respectively. Since the present measurements extend to angles large compared to the grazing angle, the extracted reaction cross sections can be considered to be relatively well determined. The reaction cross sections for the exotic isotopes were found to be larger than for ${}^4\text{He}$, reflecting the weak binding of ${}^6,8\text{He}$, which leads to large cross sections for reactions like breakup and transfer.

Plotted in Figs. 3(c) and 4(c) are the sums of the measured partial cross section for the ${}^6\text{He}+{}^{63,65}\text{Cu}$ systems. These represent, as shown in the earlier section, a sum of the fusion and transfer cross sections. The breakup cross sections were inferred from the difference between this sum and the calculated reaction cross section (ignoring the small inelastic contributions to the reaction cross sections). Breakup cross sections are thus estimated to be 210 mb and 280 mb for ${}^6\text{He}+{}^{65}\text{Cu}$ at 19.5 and 30 MeV, respectively. The uncertainty in these derived breakup cross sections was estimated to be 15%, this also includes uncertainties arising from the calculated reaction cross sections. These breakup cross sections are smaller than the neutron transfer cross sections [355(30) mb and 335(50) mb at 19.5 and 30 MeV, respectively], which form the largest contribution to the direct reaction cross section.

B. Measurements with heavy targets

As discussed in the earlier subsection, in the interaction of weakly bound nuclei with medium mass targets, the cross sections of some heavy reaction products contain contributions both from direct interactions of the valence nucleons with the target and from compound processes, making the separation of the two processes challenging. In the heavier systems studied here using Os targets, charged particle evaporation from the compound system is negligible and therefore neutron transfer reactions will lead to nuclei which are not populated in fusion evaporation. Shown in Fig. 7 is the charged particle spectrum from the ${}^6\text{He}+{}^{190}\text{Os}$ reaction in coincidence with the 186.7 keV transition in ${}^{190}\text{Os}$ (black line) and the 175.7 keV transition in ${}^{191}\text{Os}$ (gray line). These Q -value spectra which peak near $Q=0$ are also consistent with transfer followed by evaporation. This figure shows features almost identical to those for the medium mass discussed earlier. The main difference with respect to the medium mass nuclei (compare Figs. 6 and 7) is the presence of an additional contribution arising from inelastic scattering, which results in the peak near $Q=0$ in coincidence with γ rays from ${}^{190}\text{Os}$. Coincidence spectra with other Os isotopes were not observed due to limited statistics. Some technical difficulties during this part of the experiment prevented the measurement of the absolute cross section for the ${}^6\text{He}+{}^{190}\text{Os}$ system. The measured cross sections for

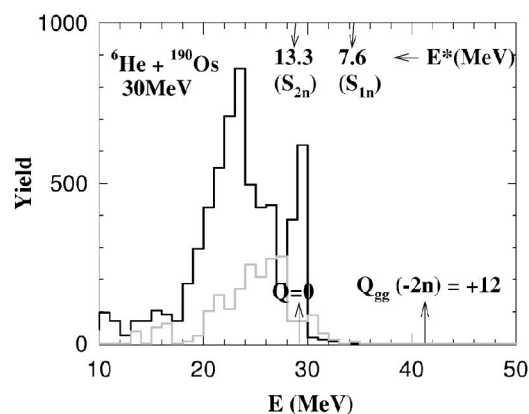


FIG. 7. Charged particles measured in the annular Si detector in coincidence with the 186.7 keV γ transition in ${}^{190}\text{Os}$ (full line) and the 175.7 keV transition in ${}^{191}\text{Os}$ (gray line) for ${}^6\text{He}+{}^{190}\text{Os}$ reaction at 30 MeV at $\theta_{lab}=37^\circ$. The yields have been corrected for efficiency and branching of the gating transition. The ground state Q values (Q_{gg}) and the neutron separation energies (S_n) in the residual nucleus in a two-neutron stripping reaction are indicated.

${}^4,6\text{He}+{}^{188,192}\text{Os}$ systems at 30 MeV are reported in Table I. As can be seen, the direct reaction cross sections with ${}^6\text{He}$, which in this case refer to the sum of inelastic and neutron transfer processes, are much larger than those with the ${}^4\text{He}$ beam. The fusion cross sections are found to be comparable for ${}^4,6\text{He}$ beams. As we will discuss later, in the present work we are unable to distinguish between complete fusion and the incomplete fusion of the alpha particle arising from breakup. It should be noted that the large cross sections for neutron transfer are a general feature with weakly bound neutron-rich nuclei and have been observed with both medium and heavy targets. Earlier measurements in the ${}^6\text{He}+{}^{209}\text{Bi}$ system were not able to detect this directly since these transfer reactions would in general populate nuclei very close to stability making any decay measurement a non optimum choice. The present measurements highlight the versatility of using the measurement of in-beam gamma rays for the detailed study of the reaction mechanism with low energy radioactive ion beams.

IV. DISCUSSION

The present measurements indicate that the neutron transfer cross sections are larger than the breakup cross sections for interactions of ${}^6\text{He}$ on medium mass targets. This assumes that all reactions where one or two neutrons are captured by the target can be labeled as transfer and not breakup followed by fusion. In the literature “breakup fusion” or even

TABLE I. Fusion and direct reaction cross sections (mb) measured for ${}^4,6\text{He}+{}^{188,192}\text{Os}$ systems at 30 MeV (see text for details).

	${}^{188}\text{Os}$		${}^{192}\text{Os}$	
	σ_f	σ_{dir}	σ_f	σ_{dir}
${}^4\text{He}$	700(70)	43(6)	789(85)	47(6)
${}^6\text{He}$	794(80)	260(35)	652(91)	260(40)

“breakup stripping” [25] reactions have sometimes been discussed, the precise definitions of these reaction mechanisms, and their differences are not straightforward to apprehend. It is not fully clear, how it will be possible to distinguish these experimentally, or even conceptually, either among themselves, or from what is generally labeled as transfer to the continuum. In this work a large cross section is observed for reactions in which one or two neutrons are captured by the target and the energy and angular characteristics of the outgoing α particle are reminiscent of a direct process. Such reactions are referred to as transfer in the present work. The other terminologies may be more appropriate for weakly bound stable projectiles like ${}^6,7\text{Li}$ which break up into two well defined charged clusters, one of which one can be captured by the target.

The measured large cross sections for this Q -matched transfer channel does imply a strong coupling strength to the elastic channel [39]. Neutron transfer reactions involving nuclei near the drip line, with large positive Q values, are expected to have a strong influence on the fusion process [45]. The present results could lead to the expectation of strong couplings to transfer channels resulting in increased fusion cross section at energies below the barrier for reactions with neutron-rich RIB’s. As mentioned earlier, the motivation of this work was to understand in a model independent way the effect of small binding energy of the valence neutrons, by means of comparison with the corresponding stable, tightly bound isotope. State of the art coupled channels calculations [2,16,17] for fusion, incorporating the effect of breakup, have not yet taken into account coupling to the transfer channel for a three-body system like ${}^6\text{He}$ with relatively large A targets. It is our intention to motivate calculations in this direction by demonstrating the possibility of such exclusive experiments (as in the present case) and the large transfer cross sections. The significant cross sections of transfer reactions with RIB’s at energies near the Coulomb barrier make it a feasible probe to investigate the structure of these weakly bound nuclei, e.g., the relative cross sections for $1n$ and $2n$ transfer could provide an insight into the spatial correlations of the valence neutrons in Borromean nuclei and pairing properties.

Investigations using weakly bound stable nuclei [3,6] have found that for reactions with heavy targets, complete fusion is “suppressed” at above barrier energies. For medium mass targets, this suppression was predicted to be smaller [7]. For reactions with RIB’s, fusion may be affected in a similar way, although the extended matter distributions of drip-line nuclei could lead to increased fusion and thus compensate for the reduction due to breakup. In the present measurement of fusion with ${}^6\text{He}$ on medium mass targets, a suppression with respect to the stable isotope is not observed. It must be noted that products from the capture of the charged fragment (${}^4\text{He}$) arising from breakup of ${}^6\text{He}$ could not be separated from the complete fusion (${}^6\text{He}+\text{Cu}$) events. The ratio of the various ER’s formed is similar in the two, given the energetics of breakup of ${}^6\text{He}$ and the Q values involved. Therefore we stress that what is labeled “fusion cross section” in the present work for ${}^6\text{He}$ projectiles is in reality the sum of the complete fusion cross section and the incomplete fusion cross section (α +target, where one or two neutrons

have escaped). This is important to consider when theoretical predictions are to be compared with the data.

In studies of fusion with weakly bound neutron-rich nuclei, capture of the neutral fragment by the target is often not considered. The present study shows that the cross section for the capture of the neutron(s) is large and arises from a direct process (transfer). These events lead to nuclei which, in the case of medium mass targets, can also be formed in complete fusion, emphasizing the need for identifying the mechanism of residue production (direct or compound) formed in reactions involving light neutron-rich RIB’s. In general it is *wrong* to equate the total residue (or fission) cross section with the fusion cross section. Figures 3(c) and 4(c) show the sum of the measured residue cross sections for the ${}^4,6\text{He}+\text{Cu}$ systems and as detailed above, for ${}^6\text{He}$ induced reactions, these include in addition to fusion a large contribution from transfer. Thus a comparison of ${}^6\text{He}$ and ${}^4\text{He}$ reactions made without separating the direct reaction contribution, would lead to erroneous conclusions about the effect of weak binding on the fusion process. In the case of nonfissioning heavy compound systems, like ${}^6\text{He}+\text{Os}$ systems, the transfer products can be easily differentiated from those formed by compound nuclear processes, as long as the charge of the residue is measured. In heavier fissioning systems the segregation of compound and direct processes also requires exclusive measurements. Recent remeasurements for the ${}^6\text{He}+{}^{238}\text{U}$ [46] system corroborate this fact, where α particles measured in coincidence with fission fragments show large cross sections for (neutron) transfer induced fission which contributed to the earlier quoted fusion-fission cross sections [10].

V. SUMMARY

In summary, we have presented results for fusion, transfer, breakup, and elastic scattering of ${}^{4,6,8}\text{He}$ on (medium mass) Cu and (heavy) Os targets near the Coulomb barrier. The feasibility of measuring small cross sections using *inclusive* in-beam γ -ray measurements with low intensity ISOL beams in conjunction with highly efficient arrays has been demonstrated. Large neutron transfer cross sections were obtained through direct measurements, and were found to be larger than those for breakup. The importance of identifying and delineating the mechanisms of residue formation for understanding fusion with RIB’s has been clearly illustrated. Kinematically complete experiments including the measurement of neutrons are now necessary to distinguish between compound and direct reactions and also between one- and two-neutron transfer processes, in order to advance toward a more complete picture of low energy reaction dynamics with neutron-rich projectiles.

ACKNOWLEDGMENTS

The authors thank the accelerator staff, G. Voltolini, and J. Ropert for their excellent technical support, and acknowledge Th. Daras of Centre de Recherches du Cyclotron, Louvain-la-Neuve for developing and providing the current amplifier. The help of R. Tripathi, S. Sodae, B. S. Tomar, and A. Mahadkar in preparation of the targets is gratefully acknowledged.

- [1] *Research Opportunities with Accelerated Beams of Radioactive Ions*, edited by I. Tanihata, special issue of Nucl. Phys. **A693** (2001).
- [2] K. Hagino, A. Vitturi, C. H. Dasso, and S. M. Lenzi, Phys. Rev. C **61**, 037602 (2000).
- [3] V. Tripathi, A. Navin, K. Mahata, K. Ramachandran, A. Chatterjee, and S. Kailas, Phys. Rev. Lett. **88**, 172701 (2002).
- [4] M. Dasgupta, D. J. Hinde, K. Hagino, S. B. Moraes, P. R. S. Gomes, R. M. Anjos, R. D. Butt, A. C. Berriman, N. Carlin, C. R. Morton, J. O. Newton, and A. Szanto de Toledo, Phys. Rev. C **66**, 041602 (2002).
- [5] C. Beck, F. A. Souza, N. Rowley, S. J. Sanders, N. Aissaoui, E. E. Alonso, P. Bednarczyk, N. Carlin, S. Courtin, A. Diaz-Torres, A. Dummer, F. Haas, A. Hachem, K. Hagino, F. Hoellinger, R. V. F. Janssens, N. Kintz, R. Liguori Neto, E. Martin, M. M. Moura, M. G. Munhoz, P. Papka, M. Rousseau, A. Sanchez i Zafra, O. Stezowski, A. A. Suaide, E. M. Szanto, A. Szanto de Toledo, S. Szilner, and J. Takahashi, Phys. Rev. C **67**, 054602 (2003).
- [6] M. Dasgupta, D. J. Hinde, R. D. Butt, R. M. Anjos, A. C. Berriman, N. Carlin, P. R. S. Gomes, C. R. Morton, J. O. Newton, A. Szanto de Toledo, and K. Hagino, Phys. Rev. Lett. **82**, 1395 (1999).
- [7] D. J. Hinde, M. Dasgupta, B. R. Fulton, C. R. Morton, R. J. Wooliscroft, A. C. Berriman, and K. Hagino, Phys. Rev. Lett. **89**, 272701 (2002).
- [8] I. Padron, P. R. S. Gomes, R. M. Anjos, J. Lubian, C. Muri, J. J. S. Alves, G. V. Marti, M. Ramirez, A. J. Pacheco, O. A. Capurro, J. O. Fernandez Niello, J. E. Testoni, D. Abriola, and M. R. Spinella, Phys. Rev. C **66**, 044608 (2002).
- [9] J. J. Kolata, Eur. Phys. J. A **13**, 117 (2002); J. J. Kolata, V. Guimaraes, D. Peterson, P. Santi, R. White-Stevens, P. A. DeYoung, G. F. Peaslee, B. Hughey, B. Atalla, M. Kern, P. L. Jolivet, J. A. Zimmerman, M. Y. Lee, F. D. Becchetti, E. F. Aguilera, E. Martinez-Quiroz, and J. D. Hinnefeld, Phys. Rev. Lett. **81**, 4580 (1998).
- [10] M. Trotta, J. L. Sida, N. Alamanos, A. Andreyev, F. Auger, D. L. Balabanski, C. Borcea, N. Coulier, A. Drouart, D. J. C. Durand, G. Georgiev, A. Gillibert, J. D. Hinnefeld, M. Huysse, C. Jouanne, V. Lapoux, A. Lepine, A. Lumbruso, F. Marie, A. Musumarra, G. Neyens, S. Ottini, R. Raabe, S. Ternier, P. Van Duppen, K. Vyvey, C. Volant, and R. Wolski, Phys. Rev. Lett. **84**, 2342 (2000).
- [11] R. Raabe *et al.*, Centre de Recherches du Cyclotron, Louvain-la-Neuve, Annual Report, 2003.
- [12] C. Signorini, Eur. Phys. J. A **13**, 129 (2002).
- [13] K. E. Rehm, H. Esbensen, C. L. Jiang, B. B. Back, F. Borasi, B. Harss, R. V. F. Janssens, V. Nanal, J. Nolen, R. C. Pardo, M. Paul, P. Reiter, R. E. Segel, A. Sonzogni, J. Uusitalo, and A. H. Wuosmaa, Phys. Rev. Lett. **81**, 3341 (2000).
- [14] A. Yoshida, C. Signorini, T. Fukuda, Y. Watanabe, N. Aoi, M. Hirai, M. Ishihara, H. Kobinata, Y. Mizoi, L. Mueller, Y. Nagashima, J. Nakano, T. Nomura, Y. H. Pu, and F. Scarlassara, Phys. Lett. B **389**, 457 (1996).
- [15] K. Zyromski, W. Loveland, G. A. Souliotis, D. J. Morrissey, C. F. Powell, O. Batenkov, K. Aleklett, R. Yanez, and I. Forsberg, Phys. Rev. C **63**, 024615 (2001).
- [16] A. Diaz-Torres and I. J. Thompson, Phys. Rev. C **65**, 024606 (2002).
- [17] A. Diaz-Torres, I. J. Thompson, and C. Beck, Phys. Rev. C **68**, 044607 (2003).
- [18] Yu. Ts. Oganessian, V. I. Zagrebaev, and J. S. Vaagen, Phys. Rev. C **60**, 044605 (1999).
- [19] A. N. Ostrowski, A. C. Shotter, S. Cherubini, T. Davinson, D. Groombridge, A. M. Laird, A. Musumarra, A. Ninane, M.-G. Pellegriti, and A. di Pietro, Phys. Rev. C **63**, 024605 (2001).
- [20] W. von Oertzen and A. Vitturi, Rep. Prog. Phys. **64**, 1247 (2001).
- [21] E. F. Aguilera, J. J. Kolata, F. M. Nunes, F. D. Becchetti, P. A. DeYoung, M. Goupell, V. Guimaraes, B. Hughey, M. Y. Lee, D. Lizzano, E. Martinez-Quiroz, A. Nowlin, T. W. O'Donnell, G. F. Peaslee, D. Peterson, P. Santi, and R. White-Stevens, Phys. Rev. Lett. **84**, 5058 (2000).
- [22] A. Di Pietro, P. Figuera, F. Amorini, C. Angulo, G. Cardella, S. Cherubini, T. Davinson, D. Leanza, J. Lu, H. Mahmud, M. Milin, A. Musumarra, A. Ninane, M. Papa, M. G. Pellegriti, R. Raabe, F. Rizzo, C. Ruiz, A. C. Shotter, N. Soic, and S. Tudisco, Europhys. Lett. **64**, 309 (2003); A. Di Pietro, P. Figuera, F. Amorini, C. Angulo, G. Cardella, S. Cherubini, T. Davinson, D. Leanza, J. Lu, H. Mahmud, M. Milin, A. Musumarra, A. Ninane, M. Papa, M. G. Pellegriti, R. Raabe, F. Rizzo, C. Ruiz, A. C. Shotter, N. Soic, S. Tudisco, and L. Weissman, Phys. Rev. C **69**, 044613 (2004).
- [23] J. J. Kolata, Phys. Rev. C **63**, 061604(R) (2001); B. R. Fulton, R. J. Wooliscroft, N. M. Clarke, and M. Freer, *ibid.* **65**, 019801 (2002); J. J. Kolata, *ibid.* **65**, 019802 (2002).
- [24] N. Keeley, J. M. Cook, K. W. Kemper, B. T. Roeder, W. D. Weintraub, F. Marchal, and K. Rusek, Phys. Rev. C **68**, 054601 (2003).
- [25] C. Signorini, A. Edifizi, M. Mazzocco, M. Lunardon, D. Fabris, A. Vitturi, P. Scopel, F. Soramel, L. Stroe, G. Prete, E. Fioretto, M. Cinausero, M. Trotta, A. Brondi, R. Moro, G. La Rana, E. Vardaci, A. Ordine, G. Inghima, M. La Commara, D. Pierrousakou, M. Romoli, M. Sandoli, A. Diaz-Torres, I. J. Thompson, and Z. H. Liu, Phys. Rev. C **67**, 044607 (2003).
- [26] J. J. Kolata, V. Z. Goldberg, L. O. Lamm, M. G. Marino, C. J. O'Keeffe, G. Rogachev, E. F. Aguilera, H. Garcia-Martinez, E. Martinez-Quiroz, P. Rosales, F. D. Becchetti, T. W. O'Donnell, D. A. Roberts, J. A. Brown, P. A. DeYoung, J. D. Hinnefeld, and S. A. Shaheen, Phys. Rev. C **65**, 054616 (2002).
- [27] R. J. Wooliscroft, N. M. Clarke, B. R. Fulton, R. L. Cowin, M. Dasgupta, D. J. Hinde, C. R. Morton, and A. C. Berriman, Phys. Rev. C **68**, 014611 (2003).
- [28] S. Chakrabarty, B. S. Tomar, A. Goswami, V. A. Raman, and S. B. Manohar, Nucl. Instrum. Methods Phys. Res. B **174**, 212 (2001).
- [29] A. C. C. Villari, Nucl. Phys. **A693**, 465 (2001).
- [30] J. Simpson, F. Azaiez, G. de France, J. Fouan, J. Gerl, R. Julin, W. Korten, P. J. Nolan, B. M. Nyako, G. Sletten, P. M. Walker, and the EXOGAM Collaboration, Acta Phys. Hung. New Ser.: Heavy Ion Phys. **11**, 159 (2000).
- [31] A. Navin, V. Tripathi, V. Nanal, Y. Blumenfeld, J. M. Casandjian, A. Chatterjee, G. de France, S. Kailas, K. Mahata, R. G. Pillay, R. Raabe, K. Ramachandran, and A. Shrivastava, in *Proceedings of the DAE Symposium of Nuclear Physics*, Tirunelveli, India (BRNS, Mumbai, 2002), Vol. 45B, p. 172.
- [32] F. Pühlhofer, Nucl. Phys. **A280**, 267 (1975).
- [33] W. N. Catford, Nucl. Phys. **A701**, 1c (2002).
- [34] S. M. Vincent, A. Aprahamian, J. J. Kolata, L. O. Lamm, V. Guimaraes, R. C. deHaan, D. Peterson, P. Santi, A. Teymura-

- zyan, F. D. Becchetti, T. W. O'Donnell, M. Lee, D. A. Roberts, J. A. Zimmerman, and J. A. Brown, *Nucl. Instrum. Methods Phys. Res. A* **491**, 426 (2002).
- [35] A. V. Ignatyuk, G. N. Smirenkin, and A. S. Tishen, *Sov. J. Nucl. Phys.* **21**, 255 (1975).
- [36] D. Wilmore and P. E. Hodgson, *Nucl. Phys.* **55**, 673 (1964).
- [37] F. D. Becchetti and G. W. Greenlees, *Phys. Rev.* **182**, 1190 (1969).
- [38] L. Mcfadden and G. R. Satchler, *Nucl. Phys.* **84**, 177 (1966).
- [39] R. A. Broglia and A. Winther, *Heavy Ion Reactions*, (Addison-Wesley, Reading, MA, 1991), Vol. 1.
- [40] M. Meister, K. Markenroth, D. Aleksandrov, T. Aumann, T. Baumann, M. J. G. Borge, L. V. Chulkov, D. Cortina-Gil, B. Eberlein, Th. W. Elze, H. Emling, H. Geissel, M. Hellstrom, B. Jonson, J. V. Kratz, R. Kulesa, A. Leistenschneider, I. Mukha, G. Munzenberg, F. Nickel, T. Nilsson, G. Nyman, M. Pfutzner, V. Pribora, A. Richter, K. Riisager, C. Scheidenberger, G. Schrieder, H. Simon, O. Tengblad, and M. V. Zhukov, *Nucl. Phys.* **A700**, 3 (2002).
- [41] M. V. Zhukov, B. V. Danilin, D. V. Fedorov, J. M. Bang, I. J. Thompson, and J. S. Vaagen, *Phys. Rep.* **231**, 151 (1993).
- [42] M. Ivascu, G. Semenescu, D. Bucurescu, and M. Titirici, *Nucl. Phys.* **A147**, 107 (1970).
- [43] J. B. A. England, S. Baird, D. H. Newton, T. Picazo, E. C. Pollacco, G. J. Pyle, P. M. Rolph, J. Alabau, E. Casal, and A. Garcia, *Nucl. Phys.* **A388**, 573 (1982).
- [44] J. Raynal, *Phys. Rev. C* **23**, 2571 (1981).
- [45] M. Dasgupta, D. J. Hinde, N. Rowley, and A. M. Stefanini, *Annu. Rev. Nucl. Part. Sci.* **48**, 401 (1998).
- [46] R. Raabe *et al.* (in preparation).